Contribution of a Conserved Asparagine to the Conformational Stability of Ribonucleases Sa, Ba, and T1[†,‡]

Eric J. Hebert,[§] Anthony Giletto,[§] Jozef Sevcik,[||] Lubica Urbanikova,[||] Keith S. Wilson,[⊥] Zbigniew Dauter,[⊥] and C. Nick Pace*[,§]

Departments of Medical Biochemistry and Genetics, Biochemistry and Biophysics and Center for Macromolecular Design, Texas A&M University, College Station, Texas 77843-1114; Institute of Molecular Biology of the Slovak Academy of Science, Dubravska cesta 21, 842 51 Bratislava, Slovak Republic, and Department of Chemistry, University of York, Heslington, York YO1 5DD, United Kingdom

Received June 26, 1998; Revised Manuscript Received September 15, 1998

ABSTRACT: The contribution of hydrogen bonding by peptide groups to the conformational stability of globular proteins was studied. One of the conserved residues in the microbial ribonuclease (RNase) family is an asparagine at position 39 in RNase Sa, 44 in RNase T1, and 58 in RNase Ba (barnase). The amide group of this asparagine is buried and forms two similar intramolecular hydrogen bonds with a neighboring peptide group to anchor a loop on the surface of all three proteins. Thus, it is a good model for the hydrogen bonding of peptide groups. When the conserved asparagine is replaced with alanine, the decrease in the stability of the mutant proteins is 2.2 (Sa), 1.8 (T1), and 2.7 (Ba) kcal/mol. When the conserved asparagine is replaced by aspartate, the stability of the mutant proteins decreases by 1.5 and 1.8 kcal/mol for RNases Sa and T1, respectively, but increases by 0.5 kcal/mol for RNase Ba. When the conserved asparagine was replaced by serine, the stability of the mutant proteins was decreased by 2.3 and 1.7 kcal/mol for RNases Sa and T1, respectively. The structure of the Asn 39 ⇒ Ser mutant of RNase Sa was determined at 1.7 Å resolution. There is a significant conformational change near the site of the mutation: (1) the side chain of Ser 39 is oriented differently than that of Asn 39 and forms hydrogen bonds with two conserved water molecules; (2) the peptide bond of Ser 42 changes conformation in the mutant so that the side chain forms three new intramolecular hydrogen bonds with the backbone to replace three hydrogen bonds to water molecules present in the wild-type structure; and (3) the loss of the anchoring hydrogen bonds makes the surface loop more flexible in the mutant than it is in wild-type RNase Sa. The results show that burial and hydrogen bonding of the conserved asparagine make a large contribution to microbial RNase stability and emphasize the importance of structural information in interpreting stability studies of mutant proteins.

Peptide groups dominate protein structure. They are exceptionally polar (*1*) but are 82% buried in folded proteins, which is not very different from the 86% observed for the nonpolar leucine side chain and considerably greater than the 55% observed for the polar amide groups of asparagine and glutamine side chains (*2*). On average, globular proteins form 1.1 hydrogen bonds per residue when they fold, and 1.0 of these are by the peptide groups. The >C═O···H−N< hydrogen bonds formed between peptide groups make up 68.1% of the hydrogen bonds, and those between peptide groups and side chains make up a further 21.3% (*3*). Thus, the hydrogen bonds of the peptide group make a far larger contribution to protein stability than the hydrogen bonds of the side chains. Unfortunately, hydrogen bonds by peptide groups are more difficult to study because they cannot be removed by mutation, and alternative strategies are needed to assess their importance. For example, Lu et al. (*4*) and Koh et al. (*5*) both conclude that the intramolecular hydrogen bonds formed by peptide groups make a favorable contribution to protein stability, but Eberhardt and Raines and colleagues (*6*) conclude that amide···water hydrogen bonds are stronger than amide···amide hydrogen bonds. The hydrogen bonding of the amide group of a conserved asparagine to a peptide unit described here provides a good model for gaining further insight into the contribution of peptide hydrogen bonds to protein stability.

RNase Sa is a small (96 amino acids) enzyme that is synthesized by *Streptomyces aureofaciens* and secreted into their growth medium (*7*). We have expressed RNase Sa in *Escherichia coli* and developed a purification procedure that yields over 50 mg of protein/L of culture medium (*8*). We have completed studies of the conformational stability and

[†] This work was supported by Slovak Academy of Sciences Grant 2/1070/96, Howard Hughes Institute Grant 75195-547601, NIH Grant GM37039, Robert A. Welch Foundation Grant A-1060, Texas Advanced Research Project Grant 010366-181, and the Tom and Jean McMullin Professorship.

[‡] The coordinates and structure factors described in this paper have been deposited in the Brookhaven Protein Data Bank under filename 1BOX.

* Corresponding author: Department of Medical Biochemistry, Texas A&M University, College Station, TX 77843-1114. Phone 409-845-1788; Fax 409-847-9481; email nickpace@tamu.edu.

[§] Texas A&M University.

[||] Institute of Molecular Biology of the Slovak Academy of Science.

[⊥] York University.

10.1021/bi9815243 CCC: $15.00
Published on Web 10/21/1998

thermodynamics of folding of RNase Sa and two close relatives, RNases Sa2 and Sa3 (*9*). RNase Sa is a member of the microbial ribonuclease family whose best studied members are RNase Ba (also known as barnase) and RNase T1 (*10, 11*). The mechanism and energetics of folding of RNases Ba (*12*) and T1 (*13, 14*) have been studied in depth, and these studies have improved our understanding of protein folding. RNases Sa, Ba, and T1 have remarkably similar structures in the β-sheet regions near the active sites, but there are substantial differences in the α-helices and turns (*9*).

There is a conserved asparagine in RNases Sa (Asn 38), T1 (Asn 44), and Ba (Asn 58). This residue is buried in a hydrophobic cluster and anchors a loop on the surface of the enzymes by forming hydrogen bonds with the carbonyl O and amide H of a peptide group as shown below in Figure 2. The hydrogen bonding of the peptide group of this conserved asparagine is important to the specificity of substrate binding (*15*), and as shown here, the side chain makes an important contribution to stability. We report studies of the conserved asparagine to alanine, serine, and aspartate mutants of RNases Sa and T1. These results are compared with studies of the Asn 58 ⟹ Ala and Asp mutants of RNase Ba previously reported by the Fersht laboratory (*16*). Our primary goal was to reach a better understanding of the contribution of hydrogen bonding, especially by peptide groups, to protein stability.

MATERIALS AND METHODS

Materials. Vent polymerase used in the polymerase chain reaction (PCR) was from New England Biolabs. All enzymes for the manipulation of DNA were from Promega Corporation. Taq polymerase cycle sequencing kit was from Perkin-Elmer Corp. Oligonucleotides were made at the 40 nM scale by Gene Technologies Laboratory at Texas A&M University and were used without further purification. All other reagents were of analytical grade or better.

Proteins. Wild-type and mutant forms of RNase Sa were expressed in the periplasmic space of *E. coli* by using the pEH100 expression vector and purified as described previously (*8*). For the expression of the RNase Sa mutants, a higher level of IPTG (1 mM) was required for maximum protein expression. Mutants of RNase Sa were made by the four-primer PCR overlapping extension technique (*17*). PCR amplification included the phoA−RNase Sa gene fusion between the *Eco*RI and *Xba*I cleavage sites in pEH100. PCR reactions contained 20 pmol of each primer, 10 ng of pEH100 target sequence, 200 mM dNTPs, and 2.5 units of Vent polymerase and were performed in 100 μL reaction volumes. The thermal cycler profile was 94 °C (1.5 min), 72 °C (2 min) for 1 cycle, followed by 25 cycles of 91 °C (1.5 min), 72 °C (2 min), and then a 7.0 min extension period at 72 °C. Putative mutants were cloned into the *Eco*RI and *Xba*I sites in the vector pEH101. Vector pEH101 is a cassette vector designed to allow easy cloning of putative PCR mutants. This vector is identical to pEH100 except that it lacks the RNase Sa gene. The vector pEH101 was created by cloning the *Sma*I/*Hin*dIII fragment containing only the functional barstar gene from pEH100 into pKK223−3 (*8*).

The Asn 44 ⟹ Ala RNase T1 mutant was prepared as described previously (*18*). The Asn 44 ⟹ Asp and Ser RNase T1 mutants were made as described for the Gly 23 ⟹ Ala mutant (*19*).

Protein concentrations were determined by use of a molar absorption coefficient at 278 nm of 12 300 M^{-1} cm^{-1} for RNase Sa (*8*) and of 19 215 M^{-1} cm^{-1} for RNase T1 (*20*). pH measurements were made on a Radiometer model 83 pH meter using a pH calibration based on two pH standards.

Stability Measurements. Thermal unfolding curves were determined by measuring the change in circular dichroism at 234 nm for RNase Sa and at 244 nm for RNase T1 of ∼0.1 mg/mL solutions in 1 cm cuvettes with an Aviv 62DS circular dichroism spectrophotometer. The temperature was increased from 5 to 80 °C in 1 °C increments (equilibration time = 1.5 min, bandwidth = 1.0 nm, and time constant = 10 s). A nonlinear least-squares analysis was used to fit the thermal denaturation data to

$$y = \{(y_f + m_f[T]) + (y_u + m_u[T])\exp[(\Delta H_m/RT)((T - T_m)/T_m)]\}/\{1 + \exp[(\Delta H_m/RT)((T - T_m)/T_m)]\} \quad (1)$$

where $y_f + m_f[T]$ and $y_u + m_u[T]$ describe the linear dependence of the pre- and posttransitional baselines on temperature, ΔH_m is the enthalpy of unfolding at T_m, and T_m is the midpoint of the thermal unfolding curve (*21*). Curve fitting was performed with MicroCal Origin curve-fitting software (MicroCal Software, Inc., Northampton, MA). The reversibility of thermal denaturation was shown to be greater than 95% in all cases.

Urea denaturation curves for RNase T1 were determined as described (*22*). A nonlinear least-squares analysis was used to fit the data to

$$y = \{(y_f + m_f[D]) + (y_u + m_u[D])\exp[m([D] - [D]_{1/2})/RT]\}/\{1 + \exp[m([D] - [D]_{1/2})/RT]\} \quad (2)$$

where y represents the observed fluorescence intensity measured at 320 nm after excitation at 278 nm with an SLM AB2 fluorescence spectrophotometer, y_f and y_u are the intercepts and m_f and m_u are the slopes of the pre- and posttransition baselines, [D] is the urea concentration, $[D]_{1/2}$ is the urea concentration at the midpoint of the curve, and m is based on the linear extrapolation model described by eq 3 (*21*). Urea denaturation curves were determined over the pH range 2.5−8.0 with the following buffers: diglycine pH 8, MOPS pH 7, MES pH 6.5−5.5, formate pH 5.0−3.5, and glycine pH 3.0−2.0.

Structure Determination. The Asn 39 ⟹ Ser mutant of RNase Sa was crystallized from a solution containing 10 mg/mL of protein in 0.1 M Tris-HCl buffer at pH 8.0. As a precipitant, PEG 6000 at a concentration of 12% in the drops and 25% in reservoir was used. For diffraction quality crystals, microseeding in hanging drop vapor equilibration was used. The crystals are in space group $P2_12_12_1$ with unit cell dimensions a = 41.49 Å, b = 46.65 Å, and c = 51.65 Å. Data were collected at room temperature from a single crystal using a Rigaku RU200 rotating anode with CuKα radiation. The data were processed with the program DENZO (*23*), and details are given below in Table 3. The structure was solved using the AMoRe program package (*24*) with the RNase Sa coordinates 1RGG from the Brookhaven Protein Data Bank as a search model (*25, 26*). The maximum likelihood program REFMAC (*27*) was combined

with an automated refinement procedure ARP (*28*). The initial *R* factor was 36%. Eight hundred ninety-five (7.5%) of the reflections were used for R_{free} cross-validation (*29*). Refinement against all data in the final step converged with an *R* of 17.6%, Table 3. There are one protein molecule and 95 water molecules in the asymmetric unit. In the wild-type structure, almost all of the residues are well-defined with low *B* factors, but in the mutant the loop containing Ser 42 has high *B* factors, reflecting a degree of flexibility in this region.

Hydrogen Bonding and Accessibility Analyses. Solvent-accessible surface area (ASA) and the hydrogen-bonding interactions in RNase Sa were analyzed with the program *pfis*—PDB file information software (Eric J. Hebert, Texas A&M University, College Station, TX). Our version of the ASA calculations in *pfis* uses a Pascal implementation of the algorithm of Lee and Richards (*30*)written for an SGI Indigo Extreme workstation, which is similar to the program ACCESS. The atomic radii of Richards (*31*), a water probe radius of 1.4 Å, and a slice width of 0.25 Å were used for all calculations.

To determine the hydrogen-bonding interactions, hydrogen atoms were added to the PDB X-ray crystal coordinate sets of RNase T1 (9RNT), RNase Ba (1RNB), RNase Sa (1RGG), and N39S RNase Sa (1BOX) using the InsightII Biopolymer module (Biosym Technologies). Nitrogen atom to hydrogen atom, oxygen atom to hydrogen atom, and carbon atom to hydrogen atom distances used were 1.03, 1.03, and 1.09 Å, respectively. For planar nitrogens in the peptide backbone and in the side chains of Arg, Asn, Gln, His, and Trp, the hydrogen atoms were positioned in the plane of the nitrogen and on the line bisecting the acute X−nitrogen−X atom angle (*32*). For His residues, hydrogen atoms were added to both the Nδ1 and Nϵ2 atoms in the same manner, and each was checked for donor and acceptor potential. For the N-terminal nitrogen and the lysine Nζ atoms, an sp^{3+} hybridization orbital was used and hydrogen atoms were positioned at gauche$^+$, gauche$^-$, and trans positions (*33*). For the Ser and Thr side chains, the hydrogen-bonding potential for the hydroxyl side chain was sampled in the gauche$^+$, gauche$^-$, and trans positions (*33*). For Tyr residues, the Cζ−OH bond has partial double-bond character, and thus hydrogen atoms were sampled for hydrogen-bonding interactions using an sp^2 hybridized OH atom and dihedral angles of 0 and 180° in the plane of the phenyl ring (*32, 33*). Hydrogens were not added to crystallographically resolved water molecules. All water molecules were retained in the coordinate sets to which hydrogen atoms were added.

Intra- and intermolecular hydrogen bonds in the coordinate sets were identified with *pfis*. Hydrogen-bonding criteria are similar to criteria used in previous hydrogen-bonding analyses (*3, 32, 34, 35*). For each protein, hydrogen bonds were identified using the following steps. (1) Distances between all potential donors and acceptors were evaluated. For a protein−protein hydrogen bonding pair, the pair was retained if the hydrogen atom to acceptor atom distance (HA distance) was <2.6 Å or the donor atom to acceptor atom distance (DA distance) was <3.6 Å. This is more lenient than the commonly used criterion of <3.5 Å for the DA distance so we generally find more hydrogen bonds with *pfis* than with the HBPLUS program of McDonald and Thornton (*35*) or the HBOND program of Stickle et al. (*3*). In protein−solvent hydrogen-bonding pairs, two separate conditions were considered. For interactions in which the donated hydrogen was from the protein, an HA distance of <2.6 Å was used, but for hydrogen-bonding pairs in which the hydrogen was donated from a water molecule, DA distance of <3.6 Å was used. (2) Hydrogen-bonding geometry was evaluated for each retained hydrogen-bonding pair from step one. Two different angle criteria were examined. The donor−hydrogen−acceptor atom angle (DHA angle) was required to be between 90° and 180°. Acceptable values for the second angle depended on the type of acceptor involved in the hydrogen-bonding pair. (a) For sp^2 hybrid orbital acceptors, the backbone carbonyl, the oxygen acceptors in the side chains of Asn, Gln, and Tyr, and the −N= acceptors in His, the hydrogen−acceptor−antecedent acceptor atom angle (HAAA angle) was required to be in the range 90−180°. (b) For sp^3 hybrid orbital acceptors, the hydroxyls of Ser and Thr, the HAAA angle was required to be in the range 60−180° (*32, 33*). A hydrogen-bonding pair was retained if both the DHA and HAAA angles were within the defined ranges. Angle values were not evaluated for all hydrogen-bonding pairs with water. For protein−solvent hydrogen bonding pairs with a protein donor, the DHA angle was determined, but the HAAA angle was not determined due to the lack of an antecedent acceptor atom. In the remaining protein−solvent hydrogen-bonding interactions involving solvent donors, neither the DHA angle nor the HAAA angle was calculated.

Table 1: Parameters Characterizing the Thermal Unfolding of RNases Sa and T1 and Three Hydrogen-Bonding Mutants at pH 7.0 in 30 MM MOPS Buffer[a]

	T_m[b] (°C)	ΔT_m[c] (°C)	ΔH_m[d] (kcal mol^{-1})	ΔS_m[e] (cal mol^{-1} K^{-1})	$\Delta(\Delta G)$[f] (kcal mol^{-1})
			RNase Sa		
wild type	48.4		92.4	287	
Asn 39 ⇒ Asp	43.2	5.2	83.5	264	1.5
Asn 39 ⇒ Ser	40.4	8.0	73.5	234	2.3
Asn 39 ⇒ Ala	40.8	7.6	70.4	224	2.2
			RNase T1		
wild type	50.8		96.6	298	
Asn 44 ⇒ Asp	45.3	5.5	84.2	264	1.6
Asn 44 ⇒ Ser	45.8	5.0	89.6	281	1.5
Asn 44 ⇒ Ala	45.6	5.2	86.8	272	1.6

[a] T_m and ΔH_m were obtained by using nonlinear least-squares to fit thermal denaturation curves to eq 1 (*22*). The error is estimated to be ± 0.5% for T_m and ± 5% for ΔH_m. [b] $T_m = T$ where $\Delta G = 0$. [c] $\Delta T_m = T_{m,wt} - T_{m,mut}$. [d] ΔH_m = enthalpy of unfolding at T_m. [e] $\Delta S_m = \Delta H_m / T_m$. [f] $\Delta(\Delta G) = \Delta T_m \Delta S_{m,wt}$ (*73*). The error in the $\Delta(\Delta G)$ values is estimated to be ±10%.

RESULTS

Thermal Denaturation. We have shown typical thermal denaturation curves for RNase Sa (*9*) and RNase T1 (*36*) and have demonstrated that both proteins unfold reversibly by a two-state mechanism. Thermal denaturation curves were determined for each of the mutants of RNases Sa and T1, and the data were analyzed as described above. The results are presented in Table 1. These data were used to estimate the difference in stability between the wild-type protein and the mutants, $\Delta(\Delta G) = \Delta G(\text{wt}) - \Delta G(\text{mutant})$, and these values are also given in Table 1. A positive $\Delta(\Delta G)$ value indicates that the mutant is less stable than wild type. In addition, thermal denaturation curves were deter-

Table 2: Parameters Characterizing the Urea Unfolding of RNase T1 and Three Hydrogen-Bonding Mutants[a]

RNase T1	$[urea]_{1/2}$ (M)	m (cal mol^{-1} M^{-1})	$\Delta G(H_2O)$[b] (kcal/mol)	$\Delta(\Delta G)$[c] (kcal/mol)
		pH = 7[d]		
wild type	5.20 ± 0.02	1170 ± 44	6.09 ± 0.23	
Asn 44 ⇒ Asp	3.54 ± 0.04	1251 ± 60	4.43 ± 0.27	2.0 ± 0.2
Asn 44 ⇒ Ser	3.60 ± 0.02	1220 ± 58	4.39 ± 0.19	1.9 ± 0.2
Asn 44 ⇒ Ala	3.51 ± 0.04	1174 ± 42	4.12 ± 0.16	2.0 ± 0.2
		pH = 2.7[e]		
wild type	3.75	1636	6.13	
Asn 44 ⇒ Asp	3.45	1656	5.71	0.5 ± 0.1

[a] $[urea]_{1/2}$ and m were obtained by using nonlinear least-squares to fit urea denaturation curves to eq 2. [b] $\Delta G(H_2O) = m[urea]_{1/2}$. [c] $\Delta(\Delta G) = \Delta[urea]_{1/2} m_{av}$, where $\Delta[urea]_{1/2} = [urea]_{1/2}$(wild type) − $[urea]_{1/2}$(mutant). At pH 7, $m_{av} = 1204 \pm 39$ cal mol^{-1} M^{-1}. At pH 2.7, $m_{av} = 1646 \pm 14$ cal mol^{-1} M^{-1}. [d] In 30 mM MOPS buffer. The values given are the average results (± standard deviation) from three urea denaturation curves. [e] In 30 mM glycine buffer. Urea denaturation curves were determined as a function of pH between pH 2 and 7 and these are the interpolated values for $[urea]_{1/2}$ and m at pH 2.7.

mined for wild-type RNase Sa and the Asn 39 ⇒ Asp mutant in the pH range 1.5−2.5. They show that $\Delta(\Delta G) = 1.0 \pm 0.2$ kcal/mol at pH 2.0. Thus, the decrease in stability for Asn 39 ⇒ Asp is smaller when the carboxyl is protonated and uncharged than when it is charged.

Urea Denaturation. The urea denaturation of RNase T1 and all of the mutants studied to date is reversible and closely approximates a two-state folding mechanism (*18*, *36*). Urea denaturation curves for RNase T1 and the three mutants of Asn 44 reported here were determined in 30 mM MOPS buffer at pH 7 and analyzed by the linear extrapolation model

$$\Delta G = \Delta G(H_2O) - m[urea] \quad (3)$$

where m is a measure of the dependence of ΔG on urea concentration and $\Delta G(H_2O)$ is an estimate of the conformational stability of the protein that assumes that the linear dependence of ΔG on urea concentration in the transition region extends to 0 M urea (*37*, *38*). The results are presented in Table 2. In addition, for wild-type RNase T1 and the Asn 44 ⇒ Asp mutant, urea denaturation curves were determined as a function of pH in the range 2.5−8.0. These data were used to calculate $\Delta(\Delta G)$ values as a function of pH. Analysis of these pH data as described elsewhere (*39*, *40*) shows that $\Delta(\Delta G)$ (pH < 3) = 0.49 ± 0.05 kcal/mol, $\Delta(\Delta G)$ (pH > 7) = 1.93 ± 0.1, and Asp 44 has a pK = 5.7 ± 0.1 in the folded protein and 4.6 ± 0.1 in the unfolded protein. The $\Delta(\Delta G)$ values are in good agreement with the results at pH 7 and pH 2.7 given in Table 2. Thus, the $\Delta(\Delta G)$ values for RNase T1 are smaller when Asp 44 is uncharged than when it is charged, and the difference is larger than for RNase Sa.

Structure of the Asn 39 ⇒ Ser mutant. The structure of the Asn 39 ⇒ Ser mutant was determined by X-ray crystallography as summarized in Table 3 (accession number 1BOX in the Brookhaven Protein Data Bank). Superposition of the Asn 39 ⇒ Ser mutant structure on wild-type RNase Sa (1RGG) based on 84 Cα atoms gave a maximum displacement of 0.46 Å and rms of 0.22 Å. Twelve Cα atoms for which the difference was greater than 0.5 Å (2σ) were excluded. The differences in positions of the Cα atoms are shown as a function of residue number in Figure 1A.

Table 3: Data Collection Parameters and Model Properties for the Asn 39 ⇒ Ser RNase Sa Mutant

(A) Data

resolution range (Å)		14.9−1.6
unique reflections		12 724
	overall	outer range (1.63−1.60 Å)
completeness (%)	92.1	57.1
$R(I)_{merge}$ (%)	5.8	47.1
$I/\sigma(I)$	30.1	1.9

(B) Model Statistics

	R factor	R_{free}
no. of reflections	11 829	895
refinement residual (%)	17.8	21.8
final R (all reflections) (%)	17.6	
REFMAC coordinate esd (Å)	0.084	0.093

	σ	deviation	parameters
bond lengths (1−2 neighbors) (Å)	0.020	0.023	755
planar torsion angles (deg)	7.0	6.1	98

average B values (Å^2)	
main chain	23.0
side chain	26.1
waters	39.7

The differences in the surface loop around Arg 63 are caused by crystal contacts and are comparable to those seen in a series of structures of RNase Sa, in which there are two molecules in the asymmetric unit (*25*). There are major differences near the mutation site especially at residues 39−43 and at Gln 47 and Ser 48. The largest difference is 3.4 Å for the Cα of Ser 42. The changes in conformation giving rise to these differences are discussed below. The average B factors for the main-chain and side-chain atoms are shown in Figure 1B,C. They reflect the increased flexibility/disorder in the loop near the site of the mutation. The first residue, Asp 1, and the side chains of Arg 40 and Glu 41 are disordered and not included in the structure.

DISCUSSION

Hydrogen-Bonding Mutants. In an unfolded protein, most of the polar groups will be hydrogen-bonded to and loosely surrounded by water molecules (*41*, *42*). In a folded protein, most of the polar groups will form at least one intramolecular hydrogen bond (*3*, *35*), and are tightly surrounded by the polar and nonpolar groups that make up the interior (*31*, *43*). An important question is whether the free energy of the polar groups is lower in the unfolded or the folded protein. Some insight can be gained by considering the model compound data shown in Table 4. The dehydration that accompanies the transfer of an uncharged, polar group from water to the vapor phase is energetically expensive. For transfer to cyclohexane, the cost is much less. This shows clearly that van der Waals interactions (*44*) between the polar groups and cyclohexane are favorable and lower the free energy of the polar group. The van der Waals interactions will be even stronger in a folded protein because the packing is much tighter than in water or cyclohexane (*43*, *45*). For transfer into octanol, the cost drops even more because now the polar groups can form hydrogen bonds with octanol and the 3.4 M water that this phase contains. If ΔG_{tr} from cyclohexane to octanol is assumed to reflect just hydrogen-bonding, the contribution is 1.4 (peptide), 1.6 (amide), 1.0 (Tyr −OH), and 1.3 (−OH) kcal/mol per hydrogen bond (*46*). These

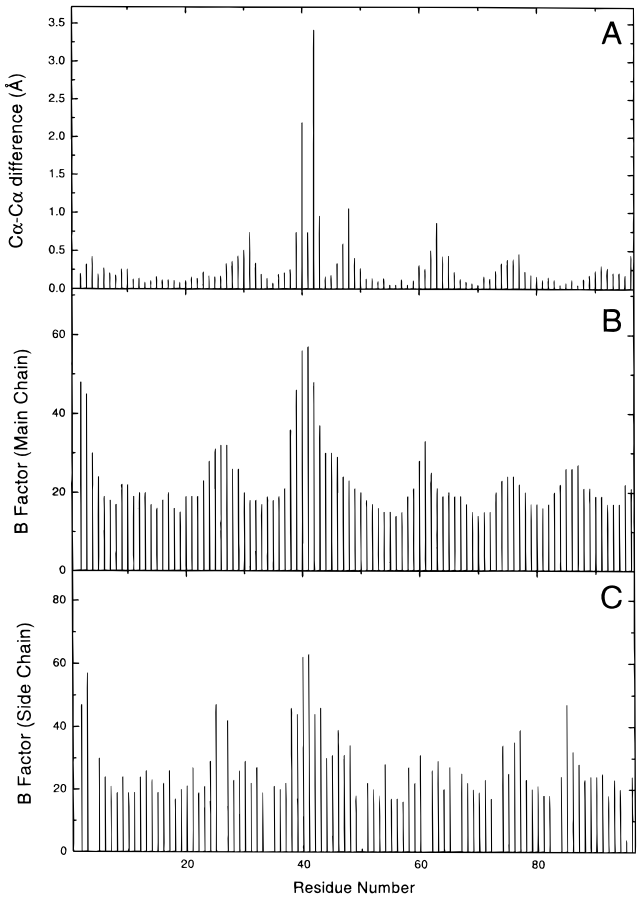

FIGURE 1: (A) Differences (in angstroms) in Cα positions between the wild-type RNase Sa (1RGG) and Asn 39 ⟹ Ser structures based on least-squares minimization of distances between 84 Cα atoms. Twelve atoms were excluded from superposition as the differences in their Cα positions were larger than 0.5 Å. The maximum difference was 3.44 Å for Ser 42 Cα. (B) Plot of average thermal parameters B (angstroms^2) for the main-chain atoms. (C) Plot of average thermal parameters B (angstroms^2) for the side-chain atoms. The increase of B values around residue 39 reflects a higher flexibility and/or a degree of disorder in this region.

Table 4: Polar Groups in Proteins[a]

	ΔG_{tr}[b] (kcal/mol)				av no. HBs[d]	
polar group	vapor	CH	oct	% buried[c]	O	H
peptide	11.7	6.4	1.1	82	1.16	0.94
amide (Asn, Gln)	11.2	7.6	1.4	55	1.25	1.35
-OH (Tyr)	7.1	3.1	1.1	67	0.52	1.06
-OH (Ser, Thr)	6.1	4.4	0.6	61	0.88	1.40

[a] ΔG_{tr} values for the transfer of the polar groups from water to vapor, cyclohexane, and *n*-octanol; average percent buried; and average number of hydrogen bonds formed in folded proteins are shown. [b] The ΔG_{tr} values are from the following sources: water to vapor (*64*); water to cyclohexane (CH) (*74*); water to *n*-octanol (oct) (*75*). The calculations were described previously (*46*). [c] The percent buried is for -CO-NH- for the peptide group, for -CO-NH_2 for asparagine and glutamine, and for -OH for tyrosine, serine, and threonine. These results are based on the structures of 61 proteins (*2*). [d] The average number of hydrogen bonds formed as an acceptor (O) and as a donor (H) is based on the structures of 57 proteins (*35*).

model compound data show that the most important forces that have to be considered are van der Waals interactions and hydrogen-bonding. Electrostatic interactions that are longer range than hydrogen bonds will make a smaller contribution.

The approach used here is to compare the stability of wild-type proteins containing a hydrogen-bonded asparagine with mutants in which the polar group has been removed (alanine) or replaced (serine and aspartate). For the asparagine to alanine mutants, both the van der Waals interactions and the intramolecular hydrogen bonds of the polar group are lost, and a hydrogen-bonding partner may be left with unfilled hydrogen bonds. For these mutations, changes in the contribution of the hydrophobic effect and conformational entropy of the side chain would be expected to stabilize the mutant (*47*). The size of the potential cavity is large for the asparagine to alanine mutation, 37.4 Å^3 (*47*). The size of the cavity is important for several reasons: (1) there is an energetic cost to pay for creating a cavity (*48*); (2) global conformational changes are more likely for larger cavities (*49*); and (3) the entry of water molecules, ≈12 Å^3, will depend on the size and polarity of the cavity (*48*). All of these factors must be considered in interpreting the results presented and have been discussed in more detail previously (*47*).

Conserved Asparagine Residue in RNases Sa, T1, and Ba. The asparagine residue considered here is conserved in 16 of 19 microbial RNases. In the species where the asparagine is not conserved, it is replaced twice by aspartate and once by alanine (*9*, *50*). The residue is buried in a hydrophobic cluster in a loop on the surface of the RNases, and the amide group forms hydrogen bonds with a peptide group (Figure 2 and Table 5). In RNase Sa, Asn 39 also forms hydrogen bonds to two water molecules and is completely hydrogen-bonded (Figure 2A). In RNase T1, a third intramolecular hydrogen bond to the −OH group of Tyr 42 (2.97 Å) replaces the hydrogen bond to the water molecule in RNase Sa (Figure 2B). In RNase Ba, the conserved asparagine forms no additional intramolecular hydrogen bonds, and there are no hydrogen bonds to water molecules (Figure 2C). A -CH_2- group from the side chain of Lys 62 takes the place of the buried water molecule in RNase Sa and the Tyr 42 -OH group in RNase T1. Thus, the hydrogen bonds between the conserved asparagine residue and a peptide group in the three proteins are very similar and provide a reasonable model for peptide−peptide hydrogen bonds. However, the other interactions of the conserved asparagine residues differ and this provides information on the context dependence of the $\Delta(\Delta G)$ values. The $\Delta(\Delta G)$ values for the replacement of these conserved asparagine residues in RNases Sa, T1, and Ba with alanine, serine, and aspartate are given in Table 5.

Asparagine to Alanine Mutants. Consider first what would be expected for this substitution if the amide group were completely buried, and no conformational change occurred in the mutant so that a 37 Å^3 cavity was formed. Xu et al. (*48*) estimate that the cost of cavity formation is 22 cal/Å^3, so this would amount to 0.8 kcal/mol favoring wild-type RNase Sa. The differences in hydrophobicity and conformational entropy between the side chains both favor the mutant and amount to ≈2.2 kcal/mol (*47*). Thus, an increase in stability of 1.4 kcal/mol would be expected, but the observed changes in stability are all *decreases* ranging from 1.8 to 2.7 kcal/mol (Table 5). This shows that the van der Waals and hydrogen-bonding interactions of the amide groups are more favorable in the folded than the unfolded protein and that the conserved asparagine makes a substantial contribution to the stability of the microbial RNases.

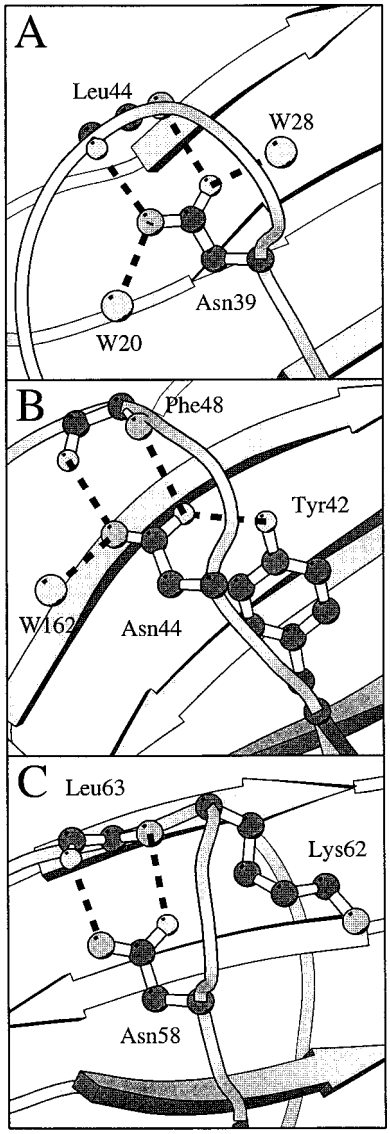

FIGURE 2: Hydrogen bonding of the conserved asparagine residue in RNases Sa (A), T1 (B), and Ba (C).

Also included in Table 5 are $\Delta(\Delta G)$ values for five other largely buried asparagine residues that form hydrogen bonds with peptide groups much like those formed by the conserved asparagine residue in the microbial RNases. The observed $\Delta(\Delta G)$ values for the eight mutants range from 1.7 to 5.1 kcal/mol, and this corresponds to a range of 0.6−1.7 kcal/mol net stabilization per intramolecular hydrogen bond. The structure of the Asn 43 ⟹ Gly mutant of bovine pancreatic trypsin inhibitor (BPTI) has been determined (*51*). The mutant structure is almost identical to that of wild-type BPTI except for the creation of a crevice at the site of the mutation. The three amide−peptide hydrogen bonds in wild type are replaced by water−peptide hydrogen bonds in the mutant. Thus, this is much like the situation described above, and the $\Delta(\Delta G) = 5.7$ kcal/mol. It is clear from these results that the burial and hydrogen-bonding of peptide groups does not just "break even" but that it makes a large favorable contribution to protein stability.

Asparagine to Serine Mutants. The $\Delta(\Delta G)$ values for the asparagine to serine mutants are remarkably similar to those for the alanine mutants (Table 5). This suggested that the serine does not form intramolecular hydrogen bonds in the mutant proteins, as expected under the assumption that no conformational changes occur. The difference in volume between an asparagine and serine side chain, ≈33 Å^3, is large enough to create a cavity in the mutant that would allow water molecules to enter and hydrogen-bond to the −OH of the serine. In fact, when the structure of the Asn 39 ⟹ Ser mutant was determined, some surprising changes in the conformation near the site of the mutation were observed (Figures 3 and 4). This illustrates the hazards involved in attempting to interpret the results of stability studies in the absence of structural information.

Table 5: $\Delta(\Delta G)$ Values for Asparagine to Alanine Mutants of Asparagines Hydrogen-Bonded to Peptide Groups

Asn	% buried[a]	DA[b]	$\Delta(\Delta G)$ (kcal/mol) Ala	Ser	Asp(−)	Asp(0)
Sa 39	94	2.91, 3.09	2.2[c]	2.3[c]	1.5[c]	0.9[d]
T1 44	85	2.90, 3.16 (2.97)	1.8[e]	1.7[e]	1.8[e]	0.5[f]
Ba 58	97	2.97, 3.16	2.7[g]		−0.5[g]	
Ba 84	91	2.94, 3.21 (3.49)	2.0[g]			
T1 81	100	2.99, 3.19, 2.96 (2.95)	2.9[h]			
BPTI 43	100	2.77, 3.04, 2.84	5.0[i]			
SN 100	100	2.85, 3.47, 2.99	5.1[j]			
SN 118	95	2.96, 2.82	1.7[j]			

[a] Percent buried for the amide group in the wild-type protein. Crystal structures: RNase Sa (1RGG), RNase T1 (9RNT), RNase Ba (1RNB), bovine pancreatic trypsin inhibitor (BPTI) (7PTI), and staphylococcal nuclease SN (1STN). [b] DA = donor to acceptor atom hydrogen-bond distance in angstroms calculated with *pfis* as described in Materials and Methods. The asparagine amide to peptide hydrogen bond distances are given first, followed in parentheses by the asparagine amide to side chain hydrogen-bond distances. [c] $\Delta(\Delta G)$ values for RNase Sa from Table 1. [d] $\Delta(\Delta G)$ value from thermal denaturation curves determined at pH 2, as described in Results. At pH 2, $T_m = 28.0$ °C and $\Delta H_m = 58.8$ kcal/mol for wild type and $T_m = 23.3$ °C and $\Delta H_m = 50.3$ kcal/mol for N39D. [e] $\Delta(\Delta G)$ values for RNase T1. The values for Asn 44 ⟹ Ser and Asp are the average of the values from Tables 1 and 2. The value for Asn 44 ⟹ Ala is the average of five values: 2.03 kcal/mol (Table 2) and 2.08 kcal/mol (*18*) from urea denaturation curves, 1.55 kcal/mol (Table 1) and 1.86 kcal/mol (*18*) from thermal denaturation curves, and 1.64 kcal/mol from DSC experiments (K. Gajiwala, unpublished results). These give $\Delta(\Delta G) = 1.83 \pm 0.23$ kcal/mol. [f] $\Delta(\Delta G)$ value from Table 2 and as described in Results. [g] $\Delta(\Delta G)$ values for the Asn 58 and 84 mutants of RNase Ba are from Serrano et al. (*16*). [h] $\Delta(\Delta G)$ value from Shirley et al. (*18*). [i] $\Delta(\Delta G)$ value from Goldenberg et al. (*76*). [j] $\Delta(\Delta G)$ value from Green et al. (*77*).

In wild-type RNase Sa, the side chain of Asn 39 forms two intramolecular hydrogen bonds to the main-chain O and N atoms of Leu 44 and two hydrogen bonds to water molecules (Figure 2A and 4A). By replacing the asparagine with serine, we hoped to see how the hydrogen-bonding and stability would be changed in the mutant enzyme. The position and side-chain conformation of Ser 39 in the mutant differs substantially from that of Asn 39 in wild type (Figures 3 and 4). The Ser 39 side chain points in a different direction, and the Oγ forms hydrogen bonds to two waters Wat 27 and Wat 86. Wat 86 is almost completely buried and forms hydrogen bonds with the backbone N and O of Gln 47. Wat 27 forms a hydrogen bond with the backbone O 47 and two water molecules Wat 8 and Wat 74. Water molecules Wat 86, Wat 27, and Wat 8 are structurally equivalent to Wat 20, Wat 21, and Wat 1 in wild-type RNase Sa but have moved 0.83, 0.62, and 0.18 Å, respectively. The resulting H-bond network is similar in the two structures. All waters are fully occupied and their thermal factors are well below the average in each structure except for Wat 86,

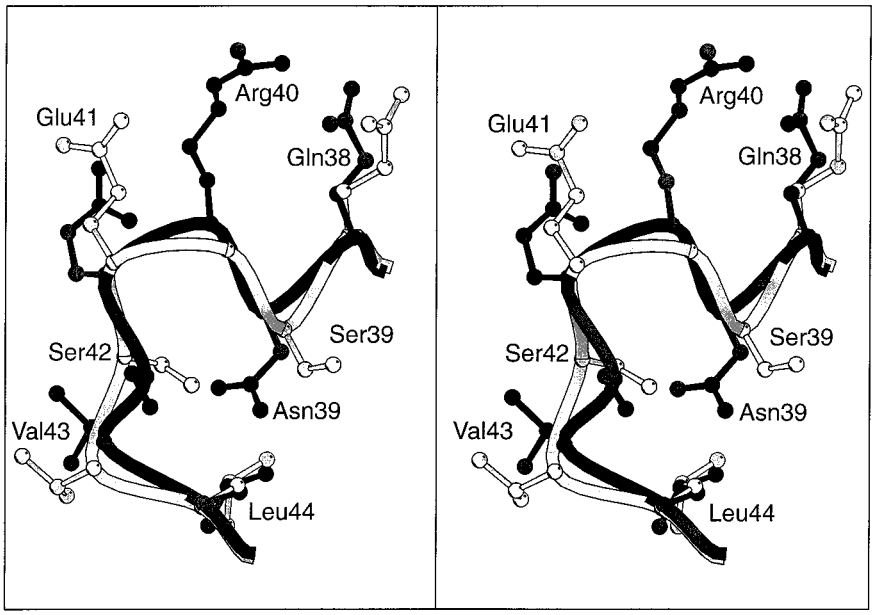

FIGURE 3: Stereoview of the structure of the main chain and side chains of the Asn 39 ⇒ Ser mutant of RNase Sa (light gray) overlapped on the wild-type structure (dark gray) near residue 39. Figure was created with MOLSCRIPT (*78*).

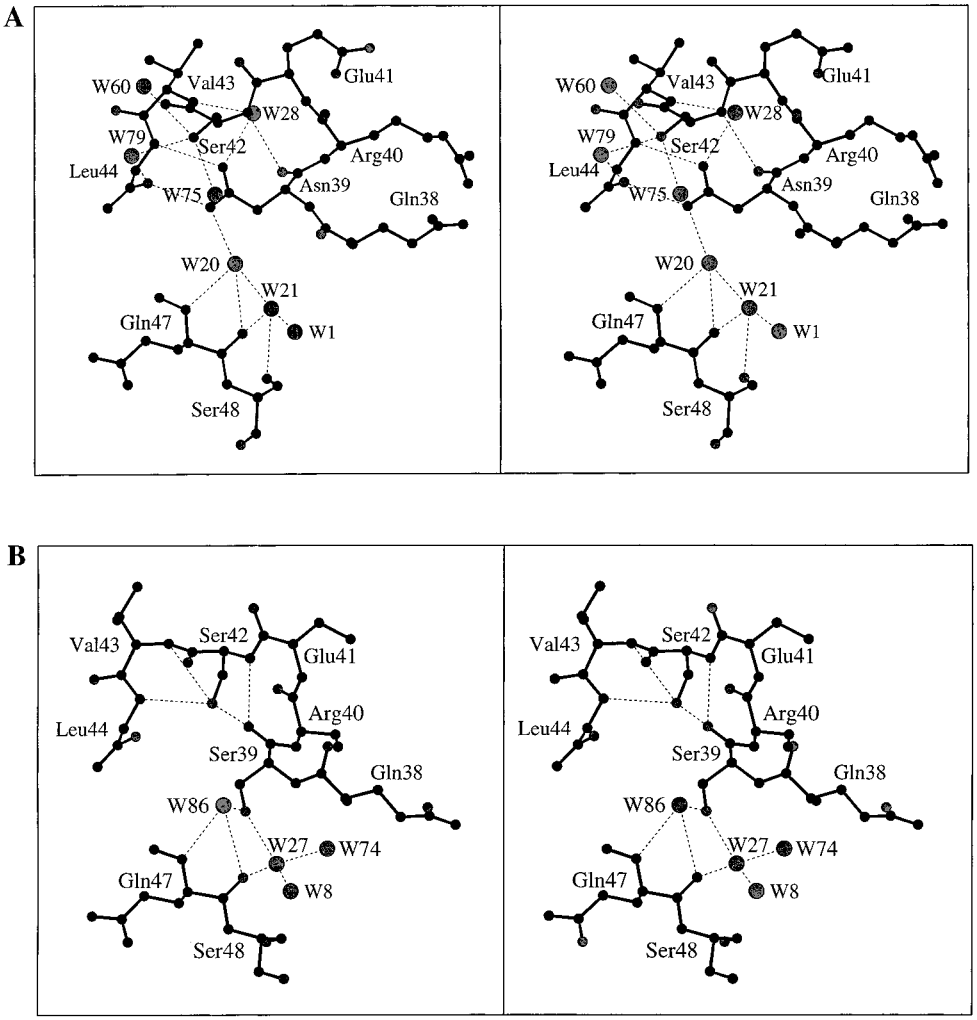

FIGURE 4: Stereoviews of wild-type RNase Sa around Asn 39 (A) and of the Asn 39 ⇒ Ser mutant around Ser 39 (B) showing differences in the hydrogen-bonding network. Figure was created with MOLSCRIPT (*78*).

which is slightly higher than the average. The new orientation of the Ser 39 side chain would create a cavity, but the peptide bond of Ser 42 changes its conformation allowing the side chain to partially fill this potential cavity and waters Wat 60, Wat 79, and Wat 28 disappear (Figure 4B). There is residual electron density in the mutant structure at the

position equivalent to Wat 79, which probably represents a solvent molecule present at partial occupancy. The Cα moves 3.4 Å and the ϕ, ψ, and χ angles change from 59.3°, 35.9°, and −158.4° in wild-type RNase Sa to −86.0°, 176.0°, and 71.0° in the Asn 39 ⟹ Ser mutant. The Ser 42 Oγ forms three intramolecular hydrogen bonds with the backbone amides of Leu 44 (3.11 Å) and Val 43 (3.22 Å) and the carbonyl O of Ser 39 (2.74 Å) to replace the three hydrogen bonds to water molecules in wild-type RNase Sa (Figure 4). There are no new water molecules in the cavity, which has instead been largely filled by the Ser 42 side chain. Thus, the substitution of serine for asparagine at position 39 causes a significant conformational change resulting in a rearrangement of the protein−protein and protein−solvent hydrogen-bonding network. When a hydrogen-bond inventory is done (*52*), there is a net loss of two hydrogen bonds: the seven hydrogen bonds in wild type (two intramolecular and five to water molecules) are replaced by five in the mutant (two intramolecular and three to water molecules). The loss in stability is ≈1.1 kcal/mol per hydrogen bond, similar to what is observed in other hydrogen-bonding mutations (*47*), but it is clear that the change in stability is the net effect of several contributing factors.

Asparagine to Aspartate Mutants. For these mutants, the p*K* of the aspartate is important. An amide group can donate two hydrogen bonds, but a carboxyl will be able to donate only one at low pH where the carboxyl is protonated and none at high pH where the carboxyl group is ionized. We were able to obtain an estimate of the p*K* of the carboxyl group in the Asn 44 ⟹ Asp mutant of RNase T1 as described in Results. The p$K = 5.7 \pm 0.1$ in the folded protein and 4.6 ± 0.1 in the unfolded protein. The unfolded p*K* value is higher than the p$K = 4.1$ expected for aspartate residues in peptides and unfolded proteins, probably because of the neighboring arginine residue (*53*−*55*). The folded p*K* value is higher than the average p$K = 2.7$ observed for aspartate residues in folded proteins (*56*). This is not surprising because this largely buried site was not designed for a carboxyl group, and the hydrogen bonding is unlikely to be optimal. As expected, the $\Delta(\Delta G)$ values are smaller at low pH where less hydrogen bonds will be lost for both RNases Sa and T1 and a charge is not buried (Table 5). At high pH where the carboxyls are ionized, the asparagine to aspartate mutants are 1.5 and 1.8 kcal/mol less stable than wild-type for RNases Sa and T1, respectively, but 0.5 kcal/mol more stable for RNase Ba. This probably reflects the fact that less hydrogen bonds are lost for RNase Ba than for RNases T1 and Sa (Figure 2) and suggests that the hydrogen bonds to the water molecules make substantial contributions to the stability in RNases T1 and Sa. Any gains in hydrogen-bond strength from the presence of a negative charge on the aspartate carboxyl are not enough to overcome the loss of the hydrogen bonds in the case of RNases T1 and Sa, but this may account for the increase in stability observed with RNase Ba. For the three microbial RNases that do not have an asparagine at this position, two have aspartate. Are there any positive charges nearby to interact with Asp 58 in this RNase Ba mutant? The Asn 58 amide group is 4.5 and 4.8 Å from the Nη1 and Nη2 groups of Arg 59 and 6.0 Å from Nζ of Lys 62. In contrast, there are no positively charged groups within 5 Å of the conserved asparagines of RNases Sa and T1. Thus, a favorable electrostatic interaction probably contributes to the stability of the RNase Ba mutant. Since asparagines occupy a volume about 10 Å^3 greater than aspartates (*45*), steric effects might contribute to the differences in stability. Thus, the asparagine to aspartate mutation at the conserved asparagine is destabilizing in RNase Sa and RNase T1 but stabilizing in RNase Ba, and the difference is probably due to a combination of effects. These results will provide a good test for the various computational methods that are used to estimate the contribution of electrostatic interactions to protein stability (*56*−*59*).

Concluding Remarks. Almost all experimental studies indicate that the intramolecular hydrogen bonds that proteins form on folding contribute favorably to protein stability (*4*, *5*, *18*, *47*, *60*−*69*), but theoretical studies suggest that they do not (*57*, *70*−*72*). The results reported here show that the hydrogen bonds between a conserved asparagine side chain and a neighboring peptide group make a large contribution to the stability of the microbial RNases. The $\Delta(\Delta G)$ values vary, but this is expected because there are differences in hydrogen bonding and the environment of the conserved asparagine residues in the three proteins. This suggests that the ≈1 hydrogen bond per residue formed by the backbone when a protein folds will make a large favorable contribution to protein stability. It will require high-resolution structural information and improvements in the theoretical approaches to sort out the relative contributions from intramolecular hydrogen bonds, intermolecular hydrogen bonds to water molecules, unfilled hydrogen bonds, and van der Waals interactions to the observed $\Delta(\Delta G)$ values. Only when computational approaches can predict conformational changes such as that observed with the Asn 39 ⟹ Ser mutant of RNase Sa will we have a good understanding of protein stability.

ACKNOWLEDGMENT

We thank Doug Laurents and members of the Pace and Scholtz lab groups for helpful discussions.

REFERENCES

1. Wolfenden, R. (1978) *Biochemistry 17*, 201−204.
2. Lesser, G. J., and Rose, G. D. (1990) *Proteins*: *Struct., Funct., Genet. 8*, 6−13.
3. Stickle, D. F., Presta, L. G., Dill, K. A., and Rose, G. D. (1992) *J. Mol. Biol. 226*, 1143−1159.
4. Lu, W., Qasim, M. A., Laskowski, M. J., and Kent, S. B. (1997) *Biochemistry 36*, 673−679.
5. Koh, J. T., Cornish, V. W., and Schultz, P. G. (1997) *Biochemistry 36*, 11314−11322.
6. Eberhardt, E. S., Wittmayer, P. K., Templer, B. M., and Raines, R. T. (1996) *Protein Sci. 5*, 1697−1703.
7. Bacova, M., Zelinkova, E., and Zelinka, J. (1971) *Biochim. Biophys. Acta 235*, 335−342.
8. Hebert, E. J., Grimsley, G. R., Hartley, R. W., Horn, G., Schell, D., Garcia, S., Both, V., Sevcik, J., and Pace, C. N. (1997) *Protein Expression Purif. 11*, 162−168.
9. Pace, C. N., Hebert, E. J., Shaw, K. L., Schell, D., Both, V., Krajcikova, D., Sevcik, J., Wilson, K. S., Dauter, Z., Hartley, R. W., and Grimsley, G. R. (1998) *J. Mol. Biol. 279*, 271−286.
10. Hill, C. P., Dodson, G. G., Heinemann, U., Saenger, W., Mitsui, Y., Nakamura, K. T., Borisov, S., Tischenko, G., Polyakov, K. M., and Pavlovsky, S. (1983) *Trends Biochem. Sci. 8*, 364−369.
11. Hartley, R. W. (1997) in *Ribonucleases structures and functions* (D'Alessio, G., and Riordan, J. F., Eds.) pp 51−100, Academic Press, Inc., New York.

12. Johnson, C. M., Oliveberg, M., Clarke, J., and Fersht, A. R. (1997) *J. Mol. Biol. 268*, 198−208.
13. Myers, J. K., Pace, C. N., and Scholtz, J. M. (1997) *Biochemistry 36*, 10923−10929.
14. Mayr, L. M., Odefey, C., Schutkowski, M., and Schmid, F. X. (1996) *Biochemistry 35*, 5550−5561.
15. Sevcik, J., Sanishvili, R. G., Pavlovsky, A. G., and Polyakov, K. M. (1990) *Trends Biochem. Sci. 15*, 158−162.
16. Serrano, L., Kellis, J. T., Cann, P., Matouschek, A., and Fersht, A. R. (1992) *J. Mol. Biol. 224*, 783−804.
17. Ho, S. N., Hunt, H. D., Horton, R. M., Pullen, J. K., and Pease, L. R. (1989) *Gene 77*, 51−59.
18. Shirley, B. A., Stanssens, P., Hahn, U., and Pace, C. N. (1992) *Biochemistry 31*, 725−732.
19. Myers, J. K., Pace, C. N., and Scholtz, J. M. (1997) *Proc. Natl. Acad. Sci. U.S.A. 94*, 2833−2837.
20. Pace, C. N., Vajdos, F., Fee, L., Grimsley, G. R., and Gray, T. (1995) *Protein Sci. 4*, 2411−2423.
21. Santoro, M. M., and Bolen, D. W. (1992) *Biochemistry 31*, 4901−4907.
22. Pace, C. N., and Scholtz, J. M. (1997) in *Protein structure: a practical approach* (Creighton, T. E., Ed.) pp 299−321, Oxford University Press, New York.
23. Otwinowski, Z., and Minor, W. (1997) *Methods Enzymol. 276*, 307−326.
24. Navaza, J., and Saludjian, P. (1997) *Methods Enzymol. 276*, 581−619.
25. Sevcik, J., Dauter, Z., Lamzin, V. S., and Wilson, K. S. (1996) *Acta Crystallogr. 52*, 327−344.
26. Bernstein, F. C., Koetzle, T. F., Williams, G. J., Meyer, E. F. J., Brice, M. D., Rodgers, J. R., Kennard, O., Shimanouchi, T., and Tasumi, M. (1977) *Eur. J. Biochem. 80*, 319−324.
27. Murshudov, G., Vagin, A., and Dodson, E. J. (1997) *Acta Crystallogr. D53*, 240−255.
28. Lamzin, V. S., and Wilson, K. S. (1997) *Methods Enzymol. 277*, 269−305.
29. Brunger, A. T. (1992) *Nature 355*, 472−475.
30. Lee, B., and Richards, F. M. (1971) *J. Mol. Biol. 55*, 379−400.
31. Richards, F. M. (1977) *Annu. Rev. Biophys. Biophys. Chem. 6*, 151−176.
32. Baker, E. N., and Hubbard, R. E. (1984) *Prog. Biophys. Mol. Biol. 44*, 97−179.
33. Ippolito, J. A., Alexander, R. S., and Christianson, D. W. (1990) *J. Mol. Biol. 215*, 457−471.
34. Presta, L. G., and Rose, G. D. (1988) *Science 240*, 1632−1640.
35. McDonald, I. K., and Thornton, J. M. (1994) *J. Mol. Biol. 238*, 777−793.
36. Thomson, J. A., Shirley, B. A., Grimsley, G. R., and Pace, C. N. (1989) *J. Biol. Chem. 264*, 11614−11620.
37. Greene, R. F. J., and Pace, C. N. (1974) *J. Biol. Chem. 249*, 5388−5393.
38. Pace, C. N. (1986) *Methods Enzymol. 131*, 266−280.
39. Stites, W. E., Gittis, A. G., Lattman, E. E., and Shortle, D. (1991) *J. Mol. Biol. 221*, 7−14.
40. Walter, S., Hubner, B., Hahn, U., and Schmid, F. X. (1995) *J. Mol. Biol. 252*, 133−143.
41. Tanford, C. (1970) *Adv. Protein Chem. 24*, 1−95.
42. Privalov, P. L., Tiktopulo, E. I., Venyaminov, S. Y., Griko, Y. V., Makhatadze, G. I., and Khechinashvili, N. N. (1989) *J. Mol. Biol. 205*, 737−750.
43. Klapper, M. H. (1971) *Biochim. Biophys. Acta 229*, 557−566.
44. London, F. (1937) *Trans. Faraday Soc. 33*, 8−26.
45. Harpaz, Y., Gerstein, M., and Chothia, C. (1994) *Structure 2*, 641−649.
46. Pace, C. N. (1995) *Methods Enzymol. 259*, 538−554.
47. Myers, J. K., and Pace, C. N. (1996) *Biophys. J. 71*, 2033−2039.
48. Xu, J., Baase, W. A., Baldwin, E., and Matthews, B. W. (1998) *Protein Sci. 7*, 158−177.
49. Matthews, B. W. (1995) *Adv. Protein Chem. 46*, 249−279.
50. Irie, M. (1997) in *Ribonucleases structures and functions* (D'Alessio, G., and Riordan, J. F., Eds.) pp 101−130, Academic Press, Inc., New York.
51. Kim, K.-S., Tao, F., Fuchs, J. A., Danishefsky, A. T., Housset, D., Wlodawer, A., and Woodward, C. (1993) *Protein Sci. 2*, 588−596.
52. Fersht, A. R. (1988) *Biochemistry 27*, 1577−1580.
53. Nozaki, Y., and Tanford, C. (1967) *J. Biol. Chem. 242*, 4731−4735.
54. Nozaki, Y., and Tanford, C. (1967) *Methods Enzymol. 11*, 715.
55. Bundi, A., and Wuthrich, K. (1979) *Biopolymers 18*, 285−297.
56. Antosiewicz, J., McCammon, J. A., and Gilson, M. K. (1996) *Biochemistry 35*, 7819−7833.
57. Sippl, M. J., Ortner, M., Jaritz, M., Lackner, P., and Flockner, H. (1996) *Folding Des. 1*, 289−298.
58. Froloff, N., Windemuth, A., and Honig, B. (1997) *Protein Sci. 6*, 1293−1301.
59. Shan, S., and Herschlag, D. (1998) *Methods Enzymol.* (*in press*).
60. Fersht, A. R., Shi, J. P., Knill-Jones, J., Lowe, D. M., Wilkinson, A. J., Blow, D. M., Brick, P., Carter, P., Waye, M. M., and Winter, G. (1985) *Nature 314*, 235−238.
61. Milla, M. E., Brown, B. M., and Sauer, R. T. (1994) *Nat. Struct. Biol. 1*, 518−523.
62. Yamada, H., Kanaya, E., Ueno, Y., Ikehara, M., Nakamura, H., and Kikkuchi, M. (1994) *Biol. Pharm. Bull. 17*, 612−616.
63. Byrne, M. P., Manuel, R. L., Lowe, L. G., and Stites, W. E. (1995) *Biochemistry 34*, 13949−13960.
64. Makhatadze, G. I., and Privalov, P. L. (1995) *Adv. Protein Chem. 47*, 307−425.
65. Huyghues-Despointes, B. M. P., Klinger, T. M., and Baldwin, R. L. (1995) *Biochemistry 34*, 13267−13271.
66. Thorson, J. S., Chapman, E., and Schultz, P. G. (1995) *J. Am. Chem. Soc. 117*, 9361−9362.
67. Habermann, S. M., and Murphy, K. P. (1996) *Protein Sci. 5*, 1229−1239.
68. Ross, P. D., and Rekharsky, M. V. (1996) *Biophys. J. 71*, 2144−2154.
69. Chapman, E., Thorson, J. S., and Schultz, P. G. (1997) *J. Am. Chem. Soc. 119*, 7151−7152.
70. Honig, B., and Yang, A. S. (1995) *Adv. Protein Chem. 46*, 27−58.
71. Yang, A. S., and Honig, B. (1995) *J. Mol. Biol. 252*, 351−365.
72. Lazaridis, T., Archontis, G., and Karplus, M. (1995) *Adv. Protein Chem. 47*, 231−306.
73. Becktel, W. J., and Schellman, J. A. (1987) *Biopolymers 26*, 1859−1877.
74. Radzicka, A., and Wolfenden, R. (1988) *Biochemistry 27*, 1644−1670.
75. Fauchere, J. L., and Pliska, V. E. (1983) *Eur. J. Med. Chem. 18*, 369−375.
76. Goldenberg, D. P., Frieden, R. W., Haack, J. A., and Morrison, T. B. (1989) *Nature 338*, 127−132.
77. Green, S. M., Meeker, A. K., and Shortle, D. (1992) *Biochemistry 31*, 5717−5728.
78. Kraulis, P. J. (1991) *J. Appl. Crystallogr. 24*, 946−950.

BI9815243